FFIBM/766/130

Approved
Kjeller October 19, 2000

Bjarne Haugstad
Director of Research

PENETRATION INTO CONCRETE BY TRUNCATED PROJECTILES

TELAND Jan Arild, SJØL Henrik

FFI/RAPPORT–2000/05292

FORSVARETS FORSKNINGSINSTITUTT
Norwegian Defence Research Establishment
Postboks 25, 2027 Kjeller, Norge

FORSVARETS FORSKNINGSINSTITUTT (FFI)
Norwegian Defence Research Establishment
P O BOX 25
NO–2027 KJELLER, NORWAY

REPORT DOCUMENTATION PAGE

1) PUBL/REPORT NUMBER	2) SECURITY CLASSIFICATION	3) NUMBER OF PAGES
FFI/RAPPORT–2000/05292	UNCLASSIFIED	22
1a) PROJECT REFERENCE	**2a) DECLASSIFICATION/DOWNGRADING SCHEDULE**	
FFIBM/766/130		

4) TITLE

PENETRATION INTO CONCRETE BY TRUNCATED PROJECTILES

(PENETRASJON I BETONG AV AVKAPPEDE PROSJEKTILER)

5) NAMES OF AUTHOR(S) IN FULL (surname first)

TELAND Jan Arild, SJØL Henrik

6) DISTRIBUTION STATEMENT

Approved for public release. Distribution unlimited
(Offentlig tilgjengelig)

7) INDEXING TERMS

IN ENGLISH:	IN NORWEGIAN:
a) Penetration	a) Penetrasjon
b) Concrete	b) Betong
c) Cavity Expansion	c) Hulromsekspansjon
d) Truncated nose	d) Avkappet nese
e)	e)

THESAURUS REFERENCE:

8) ABSTRACT

In this report we examine the penetration into semi–infinite concrete targets by truncated projectiles. Forrestal's semi–analytical penetration formula for ogive–nosed projectiles has earlier been seen to give good agreement with experiment. This formula is modified analytically to describe the penetration process for truncated projectiles, both ogive and blunt. The analytical approach is compared to an empirical modification of Forrestal's formula by Lixin et. al., where a new empirical constant was introduced. The new theory presented here introduces no new empirical constants, and is seen to agree very well with the available experimental data.

9) DATE	AUTHORIZED BY This page only	POSITION
October 19, 2000	Bjarne Haugstad	Director of Research

ISBN-82-464-0470-9

CONTENTS

Notation

a	surface area of projectile
d	diameter of projectile
d’	diameter of the flat part of the truncated nose
f	force
l	length of truncated part of the nose
m	mass of projectile
p_r	radial stress at the surface of the projectile nose
s	nose curvature radius
t	time
v_0	impact velocity
x	penetration depth
C, C_F, C_L	non–dimensional proportionality constants
F	non–dimensional force $= \frac{f}{\sigma_c d^2}$
F_0, F_1, F_2, F_2^b	non–dimensional forces
L	non–dimensional length of truncated part of the nose = $\frac{l}{d}$
M	non–dimensional mass $= \frac{m}{d^3\rho}$
N, N_0, N_2, N_2^b	nose factors
R	non–dimensional diameter $= \frac{d'}{d}$
S	non–dimensional constant in Forrestal’s formula
T	non–dimensional time $= \sqrt{\frac{d\sigma_c}{m}}t$
X	non–dimensional penetration depth $= \frac{x}{d}$
X_1	non–dimensional nose length
X_p , X_p^F , X_p^L	non–dimensional final penetration depth
V	non–dimensional velocity $V = \frac{\partial X}{\partial T} = \sqrt{\frac{m}{d^3\sigma_c}}v$
V_0	non–dimensional impact velocity
V_1	non–dimensional velocity when $X = X_1$
ϕ, ϕ_0, ϕ_1	angles defining projectile nose geometry
ρ	target density
σ_c	concrete compressive strength
ψ	non–dimensional curvature radius (CRH) = s/d

1 INTRODUCTION

Forrestal’s semi–analytical formula for penetration of rigid projectiles into concrete (1)–(2) has in various experiments been shown to give good results for different concrete qualities (3)–(4). However, the formula is only applicable for projectiles with an ogive nose. An empirical approach at extending Forrestal’s formula to truncated ogive–nosed projectiles has recently been proposed by Lixin et.al. (5). A typical projectile is depicted in Figure

1.1. However, the new theory relies on some new empirical constants and is only expected to be valid when the truncated part of the nose is less than 1/3 of the original nose length.

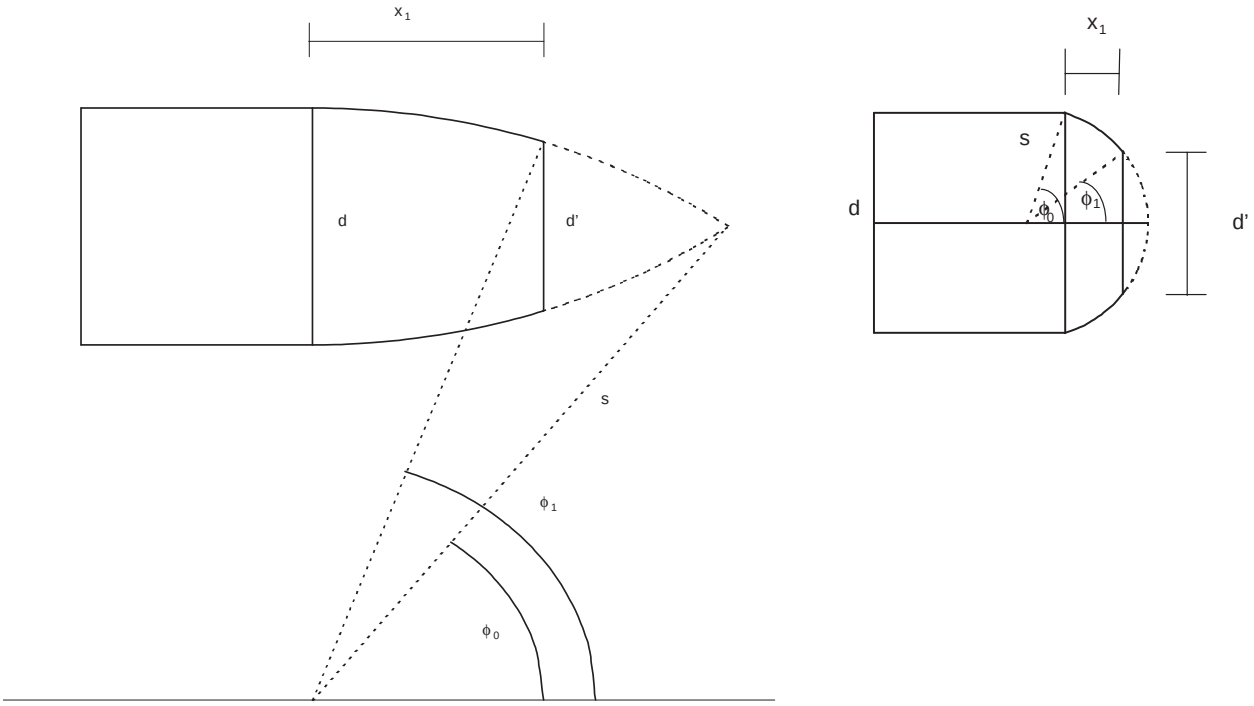

Figure 1.1: Projectile geometry

In this article, an analytical approach is used to extend Forrestal's formula to other projectile geometries, in particular all kinds of truncated noses. The new model is compared with various data and discussed.

The contents of this report has also been submitted as an article to the International Journal of Impact Engineering.

2 FORRESTAL'S FORMULA

It is convenient to introduce non–dimensional quantities for the mathematical discussion. To distinguish between quantities with and without dimension, in this paper, capital letters will always denote a non–dimensional quantity.

In Forrestal's original formulation, the penetration process is assumed to be divided into two phases. In the socalled cratering phase, when $X < 2$, the force F on the projectile is assumed proportional to the current penetration depth $X(T)$:

$$F = C_F X \quad , \quad X < 2 \tag{2.1}$$

In the cavity expansion phase, the total force decelerating the projectile is estimated according to the following integral over the projectile surface a:

$$F = \frac{1}{\sigma_c d^2} \int_a p_r(u) \cos\theta da \quad , \quad u = v\cos\theta \tag{2.2}$$

From cavity expansion theory it is possible to derive an analytical expression for p_r and thereby calculate the integral explicitly. Forrestal used a semi–analytical expression for p_r, assuming it to be on the following form:

$$p_r = S\sigma_c + \rho v^2 \quad , \quad S = 82.6\sigma_c^{-0.544} \tag{2.3}$$

where *S* is a material constant that has been experimentally determined by Forrestal. The value for the compressive strength has to be entered in MPa's since *S* is not really dimensionless, although it is assumed to be so. The expression for p_r is seen to consist of one static part and one dynamic (velocity–dependent) part.

Assuming no friction, and performing the integration gives the following expression for total force on the projectile:

$$F = \frac{\pi}{4} S\left(1 + \frac{N_0}{M}\frac{V^2}{S}\right) \quad , \quad X > 2 \tag{2.4}$$

where N_0 is a socalled nose factor only dependent on the nose geometry. For ogive and blunt noses it is given by:

$$N_0^o = \frac{8\psi - 1}{24\psi^2} \quad , \quad N_0^b = 1 - \frac{1}{8\psi^2} \tag{2.5}$$

Forrestal estimated the point of transition between the two phases from experiments. It was found that the crater depth was usually around two projectile diameters, which suggested a value of *X=2* for the transition point.

Assuming a rigid projectile together with Equations (2.1) and (2.4) for the force during penetration, enables us to apply Newton's 2nd law and calculate the complete penetration process.

The constant *C* is then determined from the requirement that *X(T), V(T)* and *F(T)* are all continuous at *X=2*. Forrestal's result is:

$$C_F = \pi\frac{S}{8}\left(1 + \frac{N_0}{M}\frac{V_1^2}{S}\right) \quad , \quad \frac{V_1^2}{S} = \frac{\frac{V_0^2}{S} - \frac{\pi}{2}}{1 + \frac{\pi}{2}\frac{N_0}{M}} \tag{2.6}$$

where V_1 is the projectile velocity at the transition point between the first and second phase.

The final penetration depth X_p^F from Forrestal's penetration formula thus becomes:

$$X_p^F = \frac{2}{\pi}\frac{M}{N_0}\ln\left(\frac{\frac{M}{N_0} + \frac{V_0^2}{S}}{\frac{M}{N_0} + \frac{\pi}{2}}\right) + 2 \tag{2.7}$$

3 MODIFICATION OF FORRESTAL'S MODEL

Here we present an attempt at generalizing Forrestal's equation to truncated projectiles. Both ogive and blunt nose shapes will be considered. The various geometrical parameters of the projectile are described in Figure 1.1.

The modification is done in two steps, first by modifying the cratering phase and then by calculating the nose factor in the second phase for such projectiles.

3.1 Where to apply the cavity expansion force?

In Forrestal's original calculation of the penetration depth, it was assumed that the cratering phase lasted until $X > 2$ when the cavity expansion phase took over. In this paper we instead propose that the transition to cavity expansion takes place when the nose has completely entered the target, i.e. when $X > X_1$, where X_1 is the non–dimensional length of the nose.

Simple geometry (see Figure 1) shows X_1 to be given by:

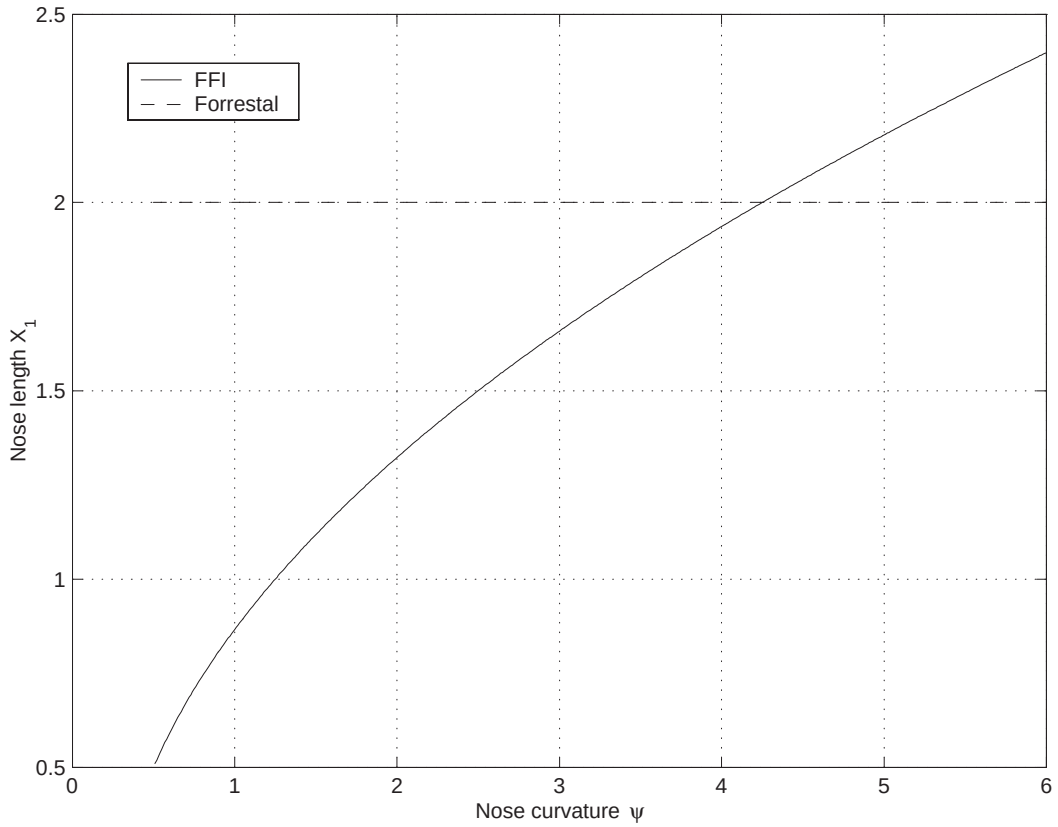

Figure 3.1: Nose length X_1 as a function of nose curvature ψ.

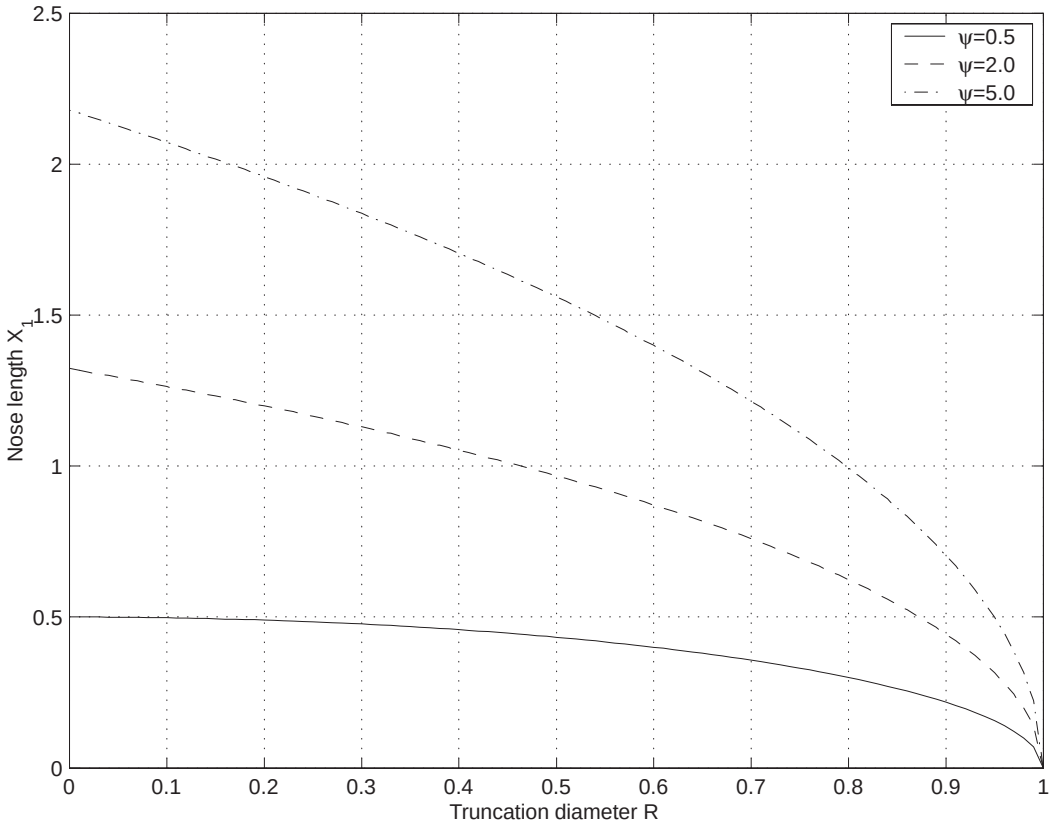

Figure 3.2: Nose length X_1 as a function of truncation diameter R.

$$X_1 = (2\psi - 1 + R)\sqrt{\frac{\psi^2}{(2\psi - 1 + R)^2} - \frac{1}{4}} \quad , \quad \psi > \frac{1}{2} \qquad (\textit{ogive nose}) \qquad (3.1)$$

$$X_1 = \sqrt{\psi^2 - \frac{R^2}{4}} - \sqrt{\psi^2 - \frac{1}{4}} \quad , \quad \psi > \frac{1}{2} \qquad (\textit{blunt nose}) \qquad (3.2)$$

In Figures 3.1 and 3.2 we have plotted X_1 as a function of ψ for *R=0* and as a function of R for different values of ψ. Our approach is consistent with Forrestal's assumption of $X_1 = 2$ as most of the projectiles in his experiments (2) had a nose length close to this value.

3.2 The force

In Forrestal's original approach, the force is zero at impact and then increases linearly with penetration depth until cavity expansion takes over. In the modified theory for truncated projectiles, a non–zero force F_0 is assumed to act on the projectile instantly after impact.

Immediately after impact, only the flat part of the projectile is in contact with the target. To calculate F_0, we use cavity expansion theory and Equation (2.2) with *u=v* (i.e. the same stress all over the surface):

$$F_0 = \frac{f_0}{\sigma_c d^2} = \pi\frac{S}{4}\left(1 + \frac{1}{M}\frac{V_0^2}{S}\right)R^2 \qquad (3.3)$$

As the nose penetrates deeper into target, there is a larger area for the stresses to act on, giving a larger force. In principle, it should be possible to apply cavity expansion at every point in time, but this would involve a time–dependent nose factor, making the equations impossible to solve analytically.

Instead we assume the force to increase linearly with the penetration depth, until $X = X_1$, when cavity expansion takes over. From various hydrocode simulations, the assumption of linearly increasing force is seen to be reasonable.

It will be shown in the next section that the final expression for the force can be written as:

$$F = \begin{cases} F_0 + CX & , \ X < X_1 \\ \pi \frac{S}{4}\left(1 + \frac{N}{M}\frac{V^2}{S}\right) & , \ X > X_1 \end{cases} \tag{3.4}$$

where N is the nose factor of the truncated projectile. For $X_1 = 2$ and $F_0 = 0$, our model is seen to reduce to Forrestal's original model.

3.3 The nose factor

In the second phase, the force decelerating the projectile is again calculated according to the integral over the projectile surface in Equation (2.2) . However, the integration is a little more complicated now and has to be divided into two parts, namely integrating over the flat part and the ogive part of the projectile.

3.3.1 Flat part

Again we find an estimate for the force F_1 on the flat part of the projectile by using Equation (2.2) with $u = v$ and integrating over the surface area of the flat part:

$$F_1 = \frac{\pi}{4} S\left(1 + \frac{1}{M}\frac{V_0^2}{S}\right)R^2 \tag{3.5}$$

It is clear that a flat nose corresponds to a nose factor *N=1*.

3.3.2 Ogive part

The force F_2 on the ogive part of the projectile is still found from cavity expansion, except that instead of integrating over the whole projectile surface, we only integrate over the ogive part of the surface, as illustrated in Figure 1.

This amounts to only integrating from ϕ_1 to $\pi/2$ instead of from ϕ_0 to $\pi/2$, where ϕ_1 and ϕ_0 are defined in Figure 1. Some simple geometry shows them to be given by:

$$\sin\phi_0 = \frac{2\psi - 1}{2\psi} \tag{3.6}$$

$$\sin\phi_1 = \frac{2\psi - 1 + R}{2\psi} \tag{3.7}$$

The expression for the force can thus be written as:

$$F_2 = 2\pi\frac{\psi^2}{\sigma_c}\int_{\phi_1}^{\pi/2} p_r(v,\phi)\left(\sin\phi - \sin\phi_0\right)\cos\phi d\phi \tag{3.8}$$

The actual calculations are now straightforward, although slightly cumbersome. In the end we obtain the following result:

$$F_2 = \frac{\pi}{4}S\left(1 - R^2\right) + \frac{1}{4}\frac{N_2}{M}V^2 \tag{3.9}$$

$$N_2 = N_0 - R^2\left(\frac{6(4\psi - 1) + 8R(1 - 2\psi) - 3R^2}{24\psi^2}\right) \tag{3.10}$$

We see that both the static and dynamic term now turn out to be functions of the normalised cavity diameter *R*.

3.3.3 Blunt part

For a blunt projectile, the force in the cavity expansion phase is given by:

$$F_2^b = 2\pi\frac{\psi^2}{\sigma_c}\int_{\phi_1}^{\phi_0} p_r(v,\phi)\sin\phi\cos\phi d\phi \tag{3.11}$$

which after integration can be written as:

$$F_2^b = \frac{\pi}{4}S\left(1 - R^2\right) + \frac{1}{4}\frac{N_2^b}{M}V^2 \tag{3.12}$$

$$N_2^b = (1 - R^2)\left(1 - \left(\frac{1 + R^2}{8\psi^2}\right)\right) \tag{3.13}$$

3.3.4 Total force

However, on adding the two force contributions F_1 and F_2 together we see that the new total force expression is identical to the old force of Equation (2.4), except for a new nose factor N in the dynamic part:

$$F = \frac{\pi}{4}S\left(1 + \frac{N}{M}\frac{V^2}{S}\right) \tag{3.14}$$

$$N = \begin{cases} N_0^o + R^2\left(\dfrac{6(2\psi - 1)^2 + 8R(2\psi - 1) + 3R^2}{24\psi^2}\right) & (\textit{ogive nose}) \\ 1 - \dfrac{(1 - R^4)}{8\psi^2} = N_0^b + \dfrac{R^4}{8\psi^2} & (\textit{blunt nose}) \end{cases} \tag{3.15}$$

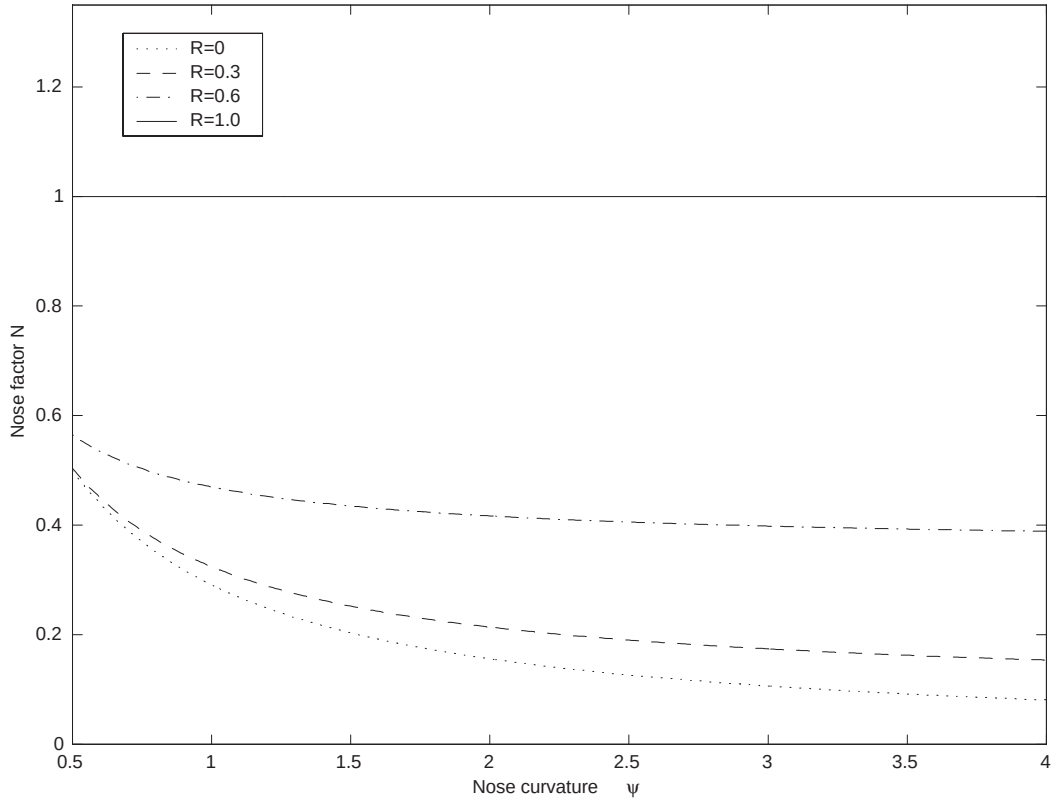

Figure 3.3: Nose factor N as a function of ψ for a truncated–ogive–projectile.

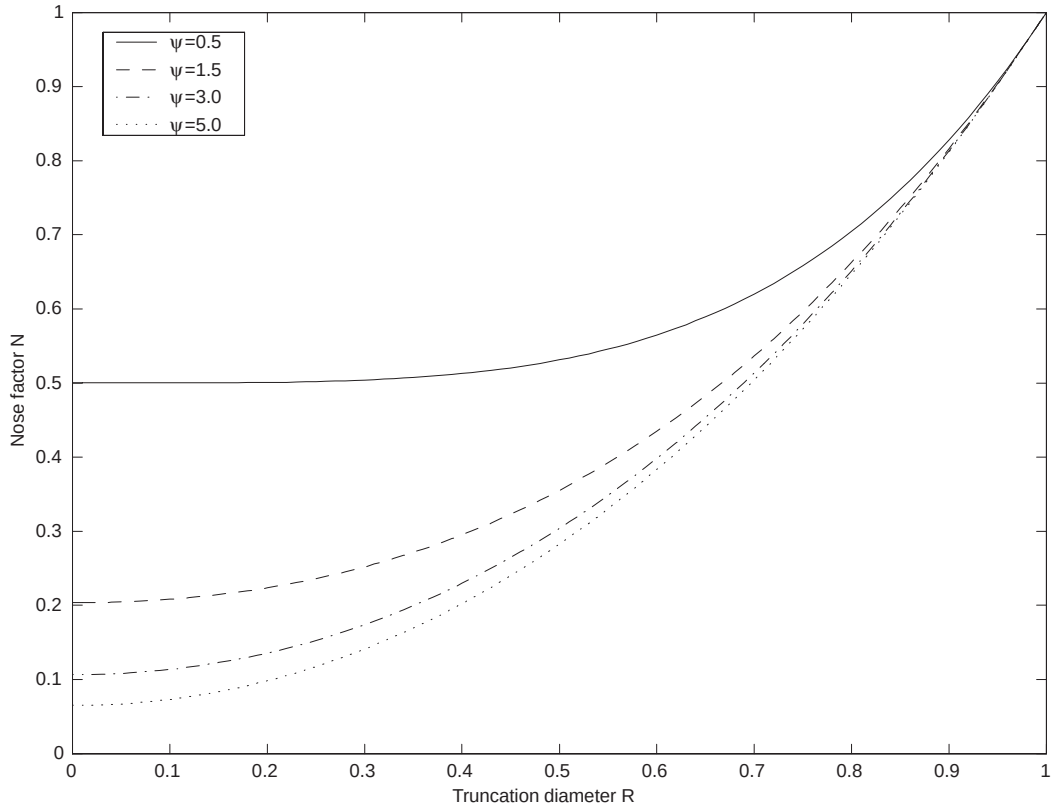

Figure 3.4: Nose factor N as a function of truncation diameter R for a truncated–ogive–projectile.

This means that the static part of the force is unaffected by the nose shape. In Figures 3.3 and 3.4 we have plotted N as a function of ψ and R respectively.

4 PENETRATION DEPTH

The final penetration depth X_p is calculated in two stages. First, the penetration depth in the cavity expansion phase is calculated as a function of a so far undetermined transition velocity V_1. This velocity is then determined from conditions of continuity at the transition point.

4.1 The cavity expansion phase

Assuming that the projectile has the velocity V_1 after the cratering phase, this velocity is used as initial condition for the cavity expansion phase. Using Newton's 2nd law and Equation (3.14) for the force, eventually gives the following relationship between X_p and V_1.

$$X_p = \frac{2}{\pi}\frac{M}{N}\ln\left(1 + \frac{N}{M}\frac{V_1^2}{S}\right) + X_1 \tag{4.1}$$

Now only an expression for V_1 as a function of the impact velocity V_0 is required. This is derived in the next section.

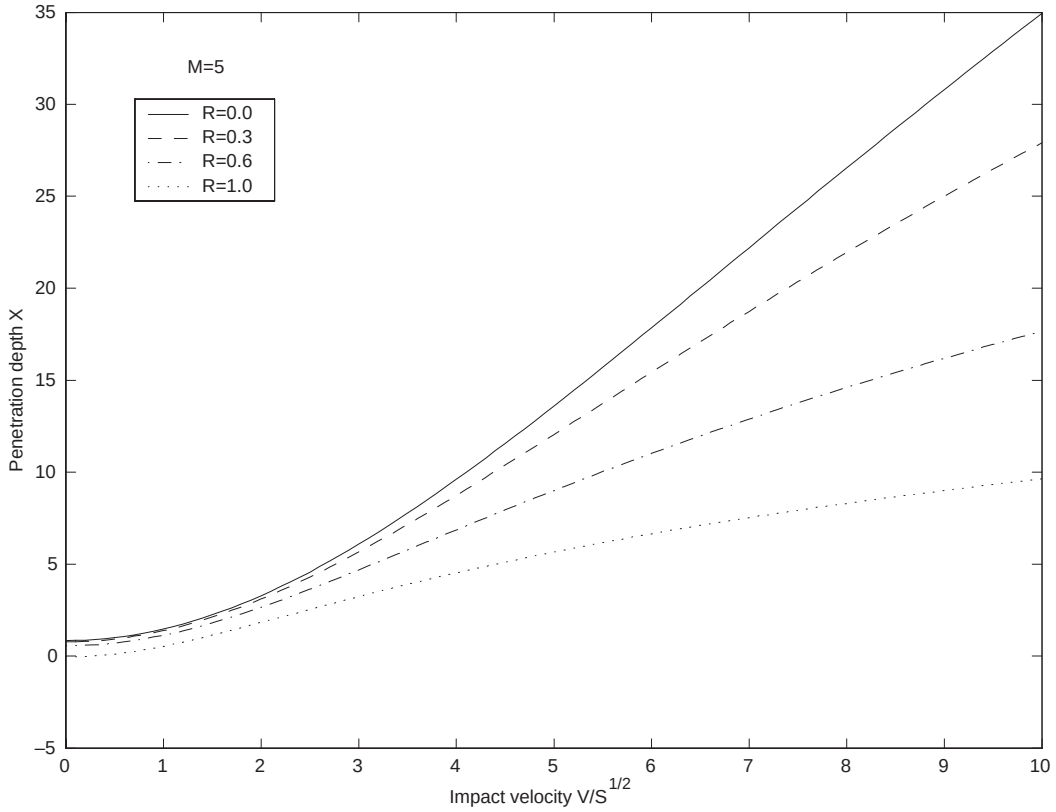

Figure 4.1: Penetration depth as a function of impact velocity.

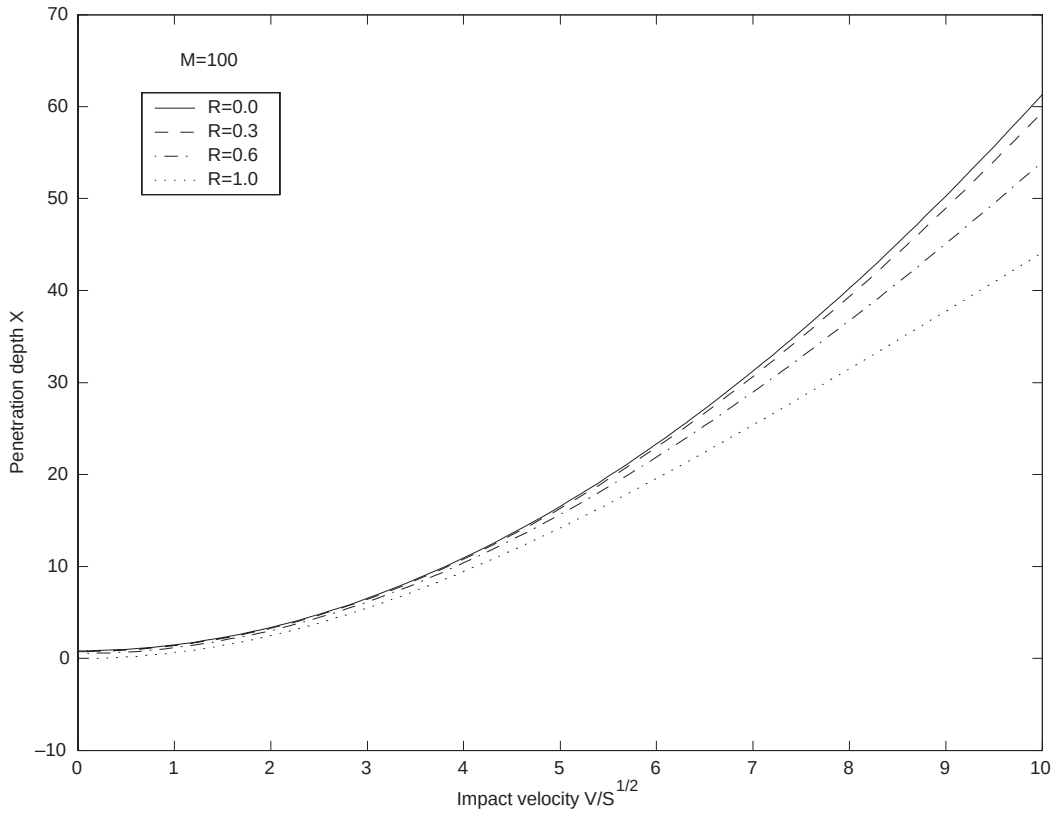

Figure 4.2: Penetration depth as a function of impact velocity.

4.2 Cratering phase

Using Newton's 2nd law on the first phase gives the following equation:

$$\frac{\partial^2 X}{\partial T^2} + CX = -\pi \frac{S}{4}\left(1 + \frac{1}{M}\frac{V_0^2}{S}\right)R^2 = -F_0 \quad , \quad X < X_1 \tag{4.2}$$

$$X(0) = 0 \quad , \quad V(0) = V_0$$

The solution of Equation (4.2) is:

$$X(T) = \frac{V_0}{\sqrt{C}}\sin\sqrt{C}\,T + \frac{F_0}{C}\left(\cos\sqrt{C}\,T - 1\right) \tag{4.3}$$

The solution from the first and final phase must be continous at $X = X_1$ in X, V and F. These conditions eventually gives us the following result:

$$C = \frac{1}{X_1^2}\left(V_0^2 - V_1^2\right) - \frac{2F_0}{X_1} \quad , \quad \frac{V_1^2}{S} = \frac{\left(1 - \frac{\pi}{4}\frac{R^2}{M}X_1\right)\frac{V_0^2}{S} - \pi\frac{X_1}{4} - \frac{\pi}{4}R^2X_1}{1 + \frac{N}{M}\frac{\pi}{4}X_1} \tag{4.4}$$

This is the generalisation of the original Equation (2.6) by Forrestal.

Inserting Equation (4.4) into Equation (4.1), we obtain the final penetration depth X_p as a function of the impact velocity V_0:

$$X_p = \frac{2}{\pi}\frac{M}{N}\ln\left[\frac{\left(1-\frac{\pi X_1 R^2}{4M}\right)\frac{V_0^2}{S}+\frac{M}{N}-\frac{\pi}{4}X_1R^2}{\frac{M}{N}+\frac{\pi}{4}X_1}\right]+X_1 \tag{4.5}$$

We see that for the special cases *R=0* and $X_1 = 2$, we retrieve Forrestal's original formula (2.7).

The penetration depth of scaled impact velocity for different values of *R* are shown in Figures 4.1 and 4.2 for *M = 5* and *M = 100*.

It is seen that for large values of *M* (roughly corresponding to long slim projectiles), there is not much difference in penetration depth whether the nose is truncated or not. However, for small values of *M*, nose shape has a large effect on penetration depth, which seems intuitively reasonable.

5 COMPARISON WITH EMPIRICAL DATA AND THEORY

In this chapter we make comparisons with empirical data and other theory.

5.1 Lixin et. al.

Lixin et.al. (5), have performed calculations for the same type of projectile. Their approach was experimental by introducing the empirical constants *C'* and X_L in the force expression:

$$F = \begin{cases} C'C_L(X+L) & , \ X < X_L \\ C'\pi\frac{S}{4}\left(1+\frac{N_0}{M}\frac{V^2}{S}\right) & , \ X > X_L \end{cases} \tag{5.1}$$

where X_L is interpreted as the the crater depth and is to be determined empirically. According to Lixin this constant is in the range between 1.5 and 2.5. In cases when no test reference is available, the Forrestal value $X_L = 2$ is supposed to be used.

The empirical constant *C'* compensates for the increased force due to the truncated nose. It is a function of the diameter of the flat part of the nose in the following way:

$$C' = 1 + KR^2 \tag{5.2}$$

By curve fitting to experiments, Lixin found the constant *K* to be given by $K = 1.5$

The constant C_L is determined from continuity conditions and takes the following form:

$$C_L = \frac{\pi}{4(X_L+L)}S\left(1+\frac{N_0}{M}\frac{V_1^2}{S}\right) \quad , \quad \frac{V_1^2}{S} = \frac{(L+X_L)\frac{V_0^2}{S}-\frac{\pi}{2}C'X_L(L+\frac{1}{2}X_L)}{L+X_L+\frac{\pi}{2}C'\frac{N_0}{M}X_L(L+\frac{1}{2}X_L)} \tag{5.3}$$

The final penetration depth X_p^L in Lixin's model then becomes:

$$X_p^L = \frac{1}{C'}\frac{2}{\pi}\frac{M}{N_0}\ln\left[\frac{\frac{V_0^2}{S}+\frac{M}{N_0}}{\frac{M}{N_0}+\frac{\pi}{4}X_L C'\left(\frac{X_L+2L}{X_L+L}\right)}\right] \tag{5.4}$$

In Figures 5.1–5.3 we have plotted the force, velocity and penetration depth as a function of time for Forrestal's Formula, Lixin's empirical approach and our analytical model for an impact velocity of 400 m/s. The values of projectile and target parameters correspond to Lixin's experiments for his 0.285 kg projetile.

It is seen that in the first phase the FFI–model predicts a larger decelerating force than the Lixin–model, while the Lixin force is stronger in the second phase. However, for the final penetration depth there is only a difference of about 5 mm.

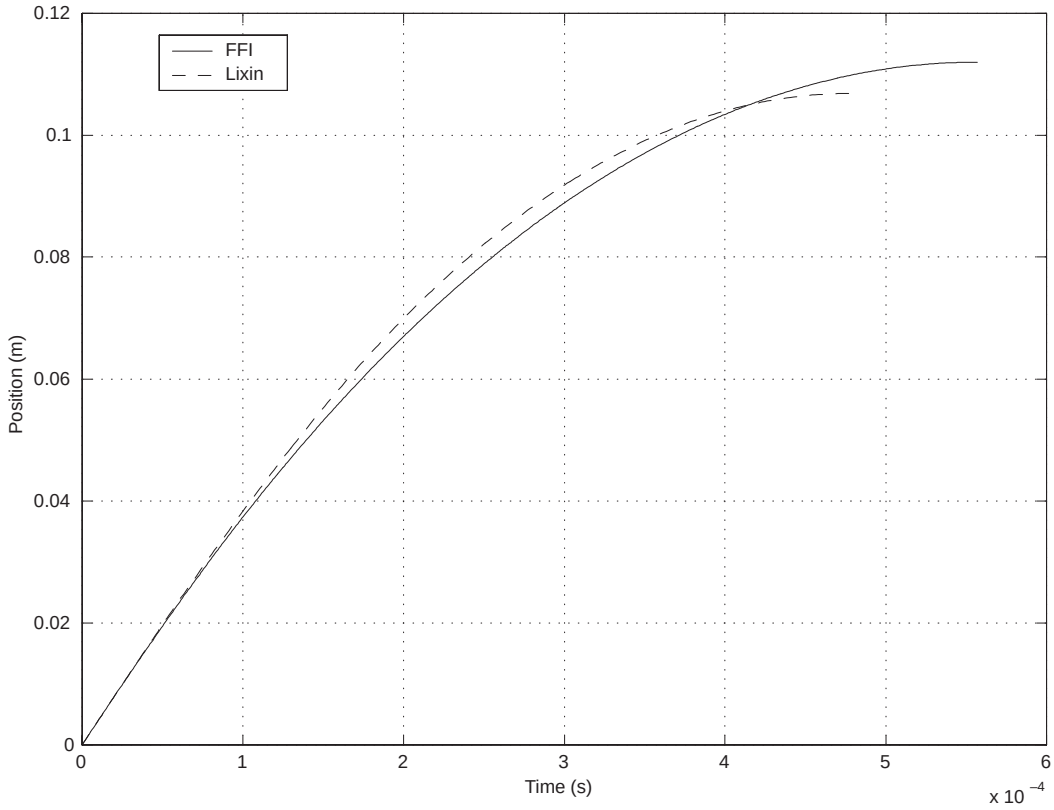

Figure 5.1: Penetration depth as a function of time.

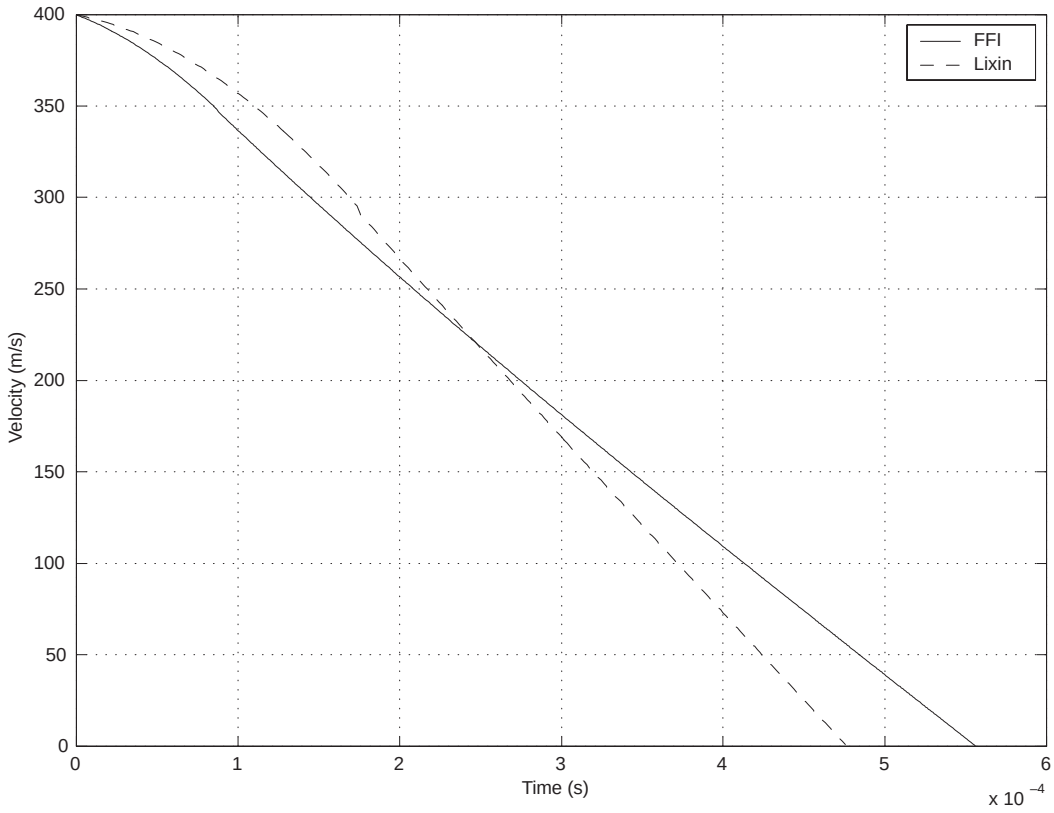

Figure 5.2: Velocity as a function of time.

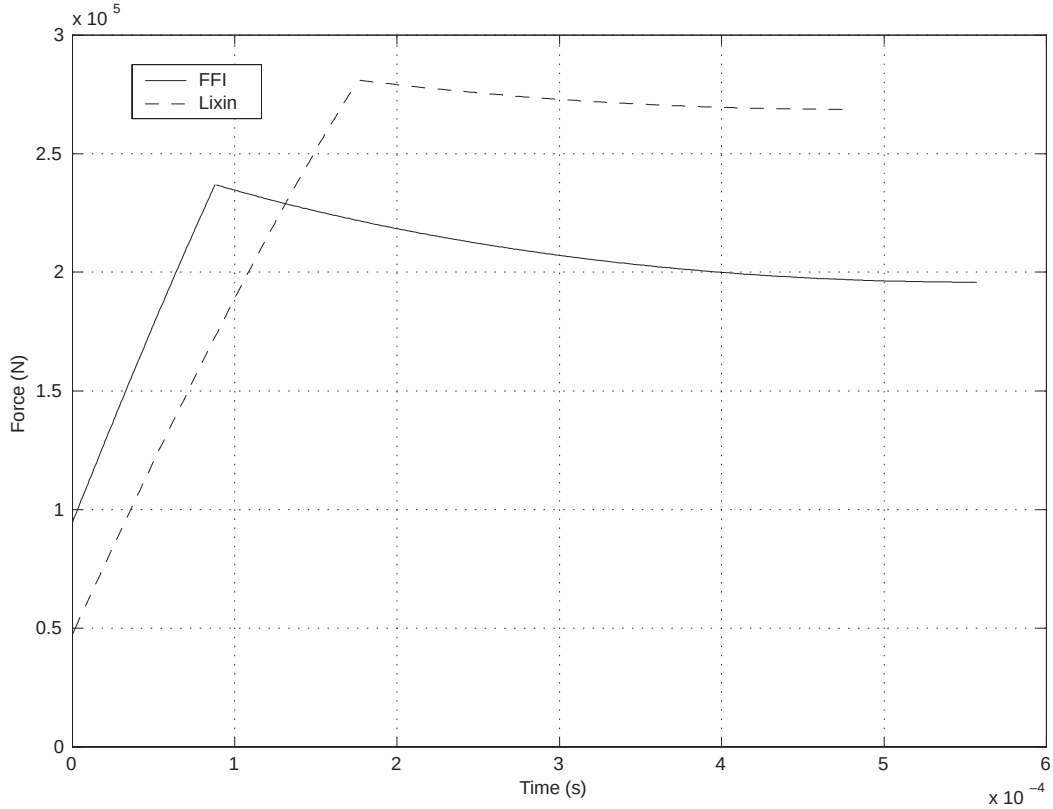

Figure 5.3: Force as a function of time.

5.2 Empirical data in Lixin et. al.

Lixin et.al. (5) have performed several penetration experiments to validate their theory. To compare our analytical theory with Lixin's data it is, however, necessary to know the concrete density, which is not given in (5). The density for a typical C–30 concrete will usually lie somewhere in the range of 2000–2500 kg/m^3. Assuming *K=2.5* and a density of 2300 kg/m^3 to enable comparison , we have plotted the penetration depth as a function of velocity for Lixin's 0.282 kg projectiles in Figure 5.4. Agreement is seen to be very good.

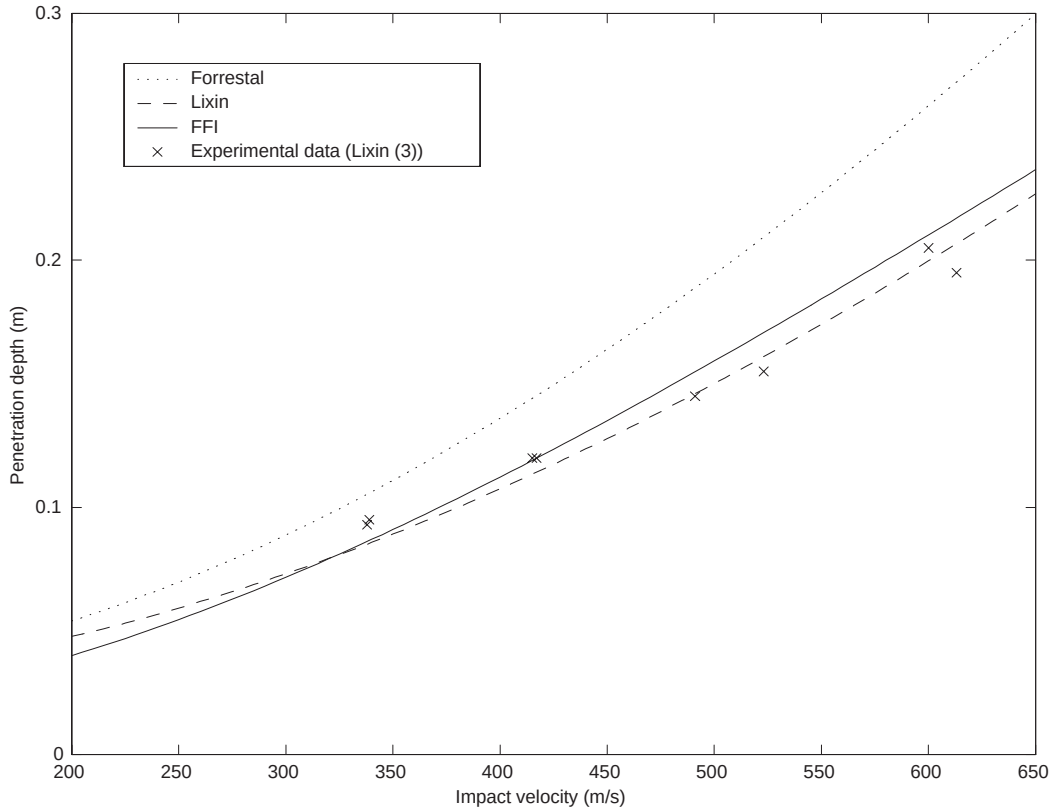

Figure 5.4: Penetration depth as a function of impact velocity.

Further, we note that our theory is not very sensitive to the concrete density and will give good agreement with experiments for any density in the range given above.

5.3 Empirical data with flat nosed projectiles

Small scale experiments with 12.7 mm flat nosed projectiles against concrete targets with compressive strength of 35 MPa were performed at FFI (6)–(7). Three different masses of the projectiles were used, namely 20.5 g, 65.8 g and 122.8 g. According to the theory discussed above, these projectiles correspond to $R = 1$ and $X_1 = 0$. The experimental results are in Figures 5.5–5.7 compared with the new FFI model and Forrestal's original model.

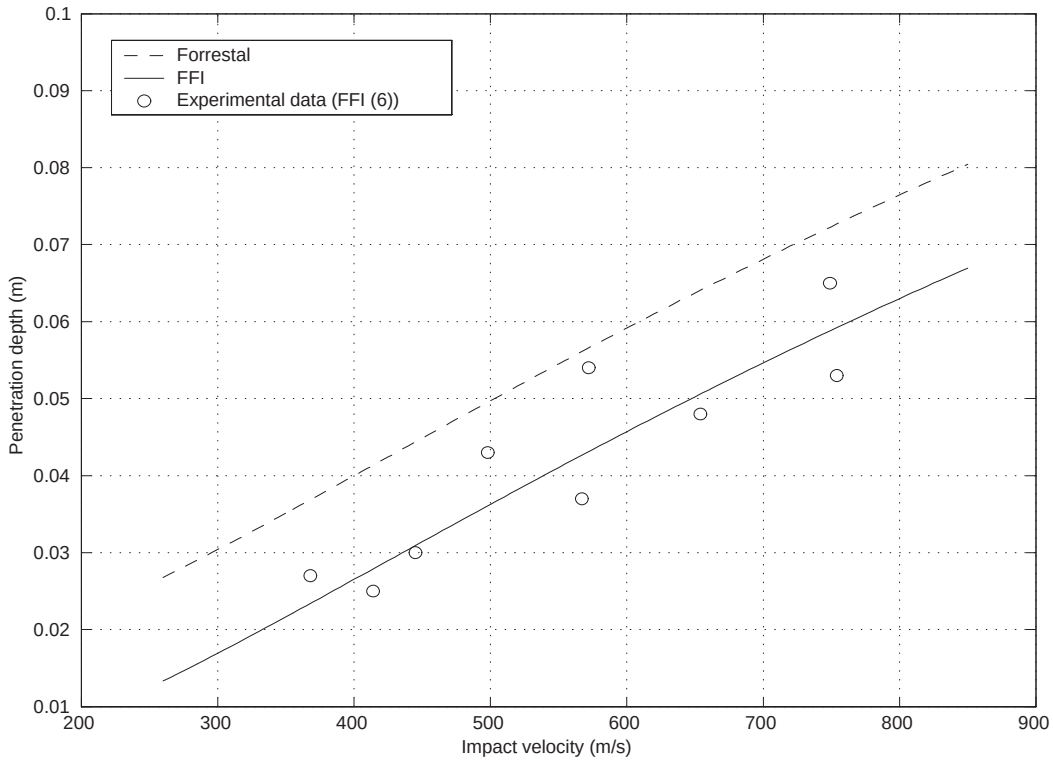

Figure 5.5: Penetration depth as a function of impact velocity for m=20.5 g projectiles.

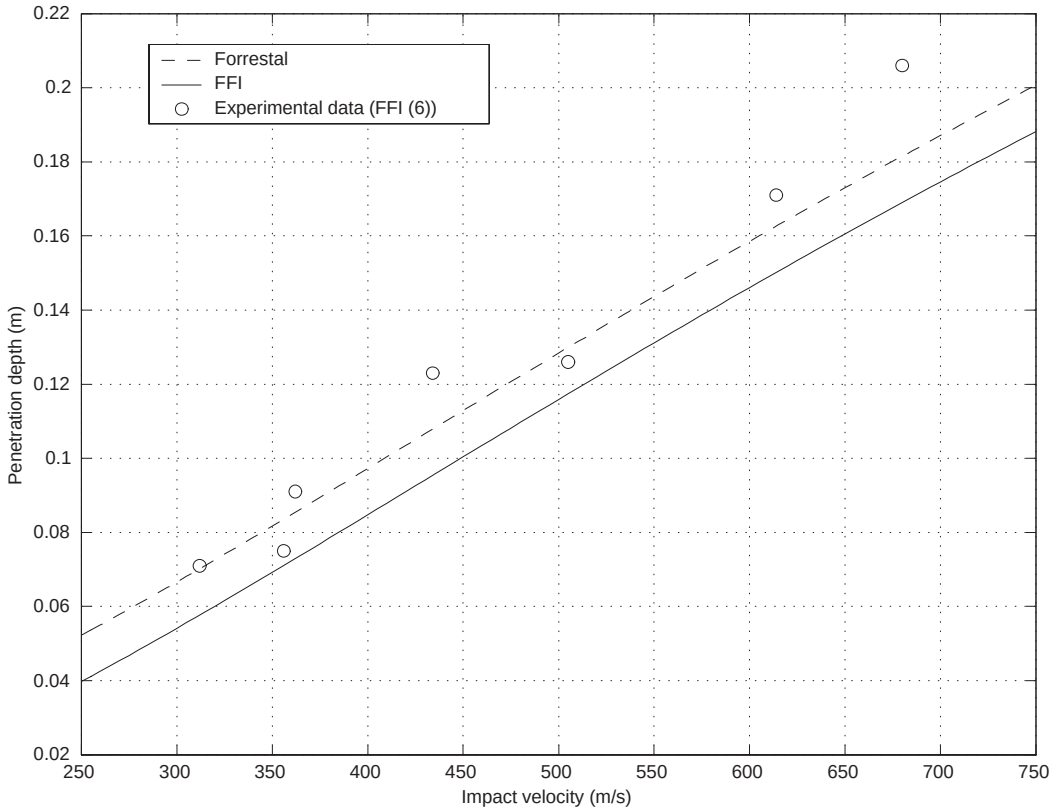

Figure 5.6: Penetration depth as a function of impact velocity for m=65.8 g projectiles.

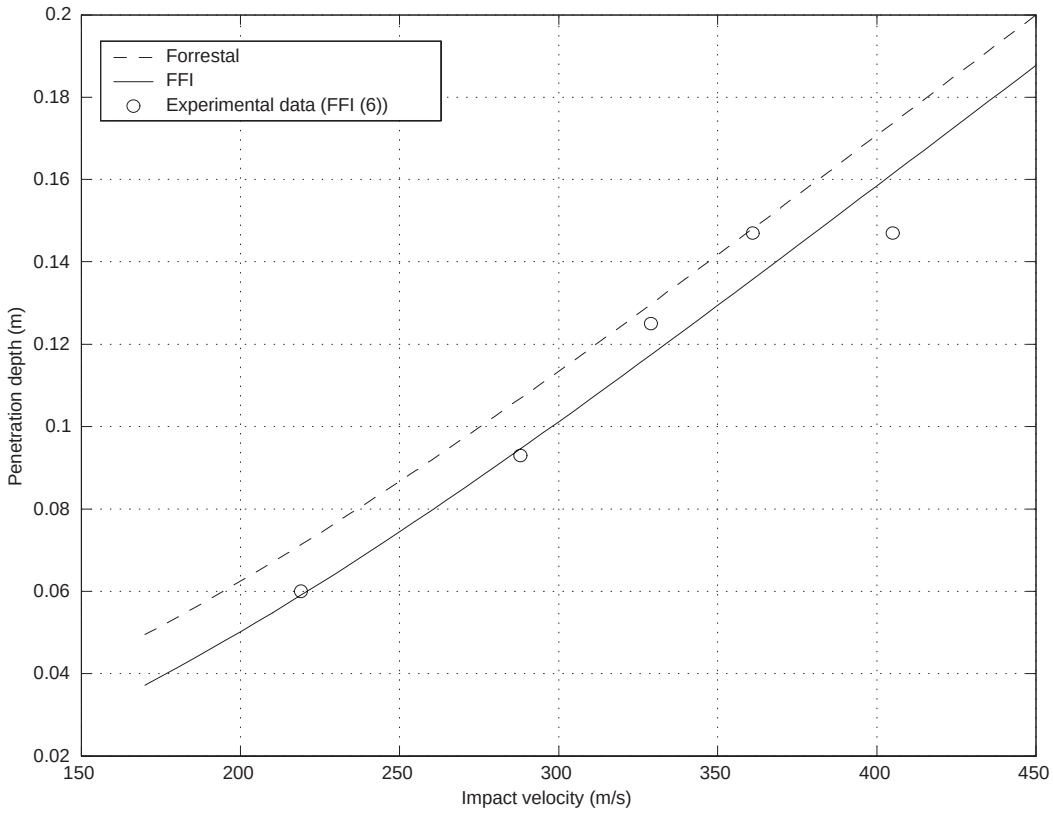

Figure 5.7: Penetration depth as a function of impact velocity for m=122.8 g projectiles.

As seen from Figures 5.5–5.7, there is very good agreement between the experimental data and the modified penetration formula given by Equation (4.5), especially for the 20.5 g and 122.8 g projectiles. The experiments with the 65.8 g projectiles seem to be slightly above the FFI–model, but the difference should be within experimental uncertainty.

The experiments with flat nosed projectiles are not compared to Lixin's model, because according to Lixin (5), the model is not valid for such projectiles. The force expression in Equation (5.1) will be too large due to the factor *C'*, which takes the value of 2.5 for flat projectiles. Hence the final penetration depth will be too small compared to the experiments.

5.4 Predrilled cavities

For completeness we note that if we put $F_0 = 0$ and $N = N_2$ in Equation (3.4) we obtain a model for penetration into targets with predrilled cavities. This topic is further discussed in (8).

6 DISCUSSION

We have modified Forrestal's semi–analytical penetration formula to obtain a new model that is valid for a larger range of projectiles. More precisely the new model is valid for projectiles of arbitrary nose length and for truncated noses. Further, it is not dependent on any new empirical factors and it shows very good agreement with various experimental data.

References

(1) Forrestal M J, Altman B S, Cargile J D, Hanchak S J, An empirical equation for penetration depth of ogive nose projectiles into concrete targets, Int J Impact Engng Vol. 15, No. 4, pp. 395–405, 1994

(2) Frew D J, Hanchak S J, Green M L, Forrestal M J, Penetration of concrete targets with ogive–nosed steel rods, Int J Impact Engng Vol. 21, No. 6, pp. 489–497, 1998

(3) Sjøl H, Teland J A, Prediction of concrete penetration using Forrestal's formula, FFI/RAPPORT–99/04415

(4) Sjøl H, Penetration of rigid projectiles into concrete targets, Submitted to Int J Impact Engng

(5) Lixin Q, Yunbin Y, Tong L, A semi–analytical model for truncated–ogive–nose projectiles penetration into semi–infinite concrete targets, Int J Impact Engng 24 (2000), pp. 947–955

(6) Sjøl H, Teland J A, Kaldheim Ø, Penetration into concrete – Experiments with 12 mm Projectiles, FFI/RAPPORT–2000/04414

(7) Sjøl H, Teland J A, Kaldheim Ø, Penetrasjon i betong med 12 mm prosjektiler, FFI/NOTAT–98/0432 (in Norwegian)

(8) Teland J A, Cavity expansion theory applied to penetration of targets with predrilled cavities, Int Ballistic Symposium 2001

DISTRIBUTION LIST

FFIBM **Dato:** 19 oktober 2000

RAPPORT TYPE (KRYSS AV)	RAPPORT NR	REFERANSE	RAPPORTENS DATO
X RAPP ☐ NOTAT ☐ RR	2000/05292	FFIBM/766/130	19 oktober 2000

RAPPORTENS BESKYTTELSESGRAD	ANTALL EKS UTSTEDT	ANTALL SIDER
UNCLASSIFIED	47	22

RAPPORTENS TITTEL	FORFATTER(E)
PENETRATION INTO CONCRETE BY TRUNCATED PROJECTILES	TELAND Jan Arild, SJØL Henrik

FORDELING GODKJENT AV FORSKNINGSSJEF:	FORDELING GODKJENT AV AVDELINGSSJEF:

EKSTERN FORDELING

ANTALL	EKS NR	TIL
1		FBT/S
1		Helge Langberg
1		Gro Markeset
1		Leif Riis
1		Anders Carlberg
1		Lennart Ågårdh
1		Håkan Hansson
1		Mattias Unosson
1		Johan Magnusson
1		FOA S–14725 TUMBA, Sverige
1		Ingvar Anglevik HKV/KRI Plan/Anläggning SE–10785 STOCKHOLM Sverige
1		Bjørn Lindberg Forv–M S–63189 ESKILSTUNA Sverige
1		Jaap Weerheijm
1		Cyril Wentzel
1		TNO Lange Kleinweg 137 P.O.Box 45 2280 AA RIJSWIJK Nederland

INTERN FORDELING

ANTALL	EKS NR	
14		FFIBIBL
1		Adm direktør/stabssjef
1		FFIE
1		FFISYS
5		FFIBM
1		Bjarne Haugstad, FFIBM
1		Svein Rollvik, FFIS
1		Eirik Svinsås, FFIBM
1		Haakon Fykse, FFIBM
1		Harald H Soleng, FFIBM
2		Henrik Sjøl, FFIBM
2		Jan Arild Teland, FFIBM

FFI–K1 Retningslinjer for fordeling og forsendelse er gitt i Oraklet, Bind I, Bestemmelser om publikasjoner for Forsvarets forskningsinstitutt, pkt 2 og 5. Benytt ny side om nødvendig.

EKSTERN FORDELING

INTERN FORDELING

ANTALL	EKS NR	TIL	ANTALL	EKS NR
1		Cathy O'Carroll		
1		Jim Sheridan		
1		DERA X107, Barnes Wallis Building Farnborough Hampshire GU14 0LX England		
1		Frikkie Mostert Somchem, a division of Denel P O Box 187 Somerset West 7129 South Africa		
1		Qian Lixin Institute of Structural Mechanics China Academy of Eng. Physics P.O. Box 919 – 414 Mianyang 621900 Sichuan China		